

Progress Report on Radiation Dosimetry Standards at NMIJ/AIST and Photon Energy Spectra Measured in Fukushima

Norio Saito, Tadahiro Kurosawa, Masahiro Kato,
Yuichiro Morishita, Takahiro Tanaka, and Morihito Shimizu
Ionizing Radiation Section, Quantum Radiation Division
National Metrology Institute of Japan (NMIJ)
National Institute of Advanced Industrial Science and Technology (AIST)
Tsukuba 305-8568, Japan

1. Introduction

We disseminate air-kerma standards for low-energy X-rays, medium-energy X-rays, mammography beams (Mo/Mo, Mo/Rh, and Rh/Rh), and gamma-rays (Co-60 and Cs-137); the standards of absorbed dose to water in a Co-60 gamma beam; and the absorbed dose to tissue for beta-rays as national primary standards. We also provide pulse energies of the X-ray free electron laser (4–20 keV). We have been developing the absorbed dose to water in high-energy photons and electrons from a Clinical linac, the air kerma standards for the high dose rate (HDR) brachytherapy of Ir-192, and the absorbed dose to water standards for beta-rays emitted from Ru-106.

In addition, we have measured the gamma-ray energy spectra in Fukushima before and after the decontamination of the ground.

2. Recent progress in development of standards

2-1. Absorbed dose rate to water in a Co-60 γ -ray field

The national standard for the absorbed dose (rate) to water in a cobalt 60 gamma-ray field at NMIJ [1] was compared with that at the International Bureau of Weights and Measures (BIPM) in 2009. NMIJ uses a graphite calorimeter as shown in Figure 1. Two farmer-type ionization chambers (PTW TN-30013 and Exradin A12) were used as transfer chambers and their calibration coefficients at a reference condition (5 cm depth in water, 20 °C, 1 atm, and 50% humidity) were compared with each other. The result [2] showed that the calibration

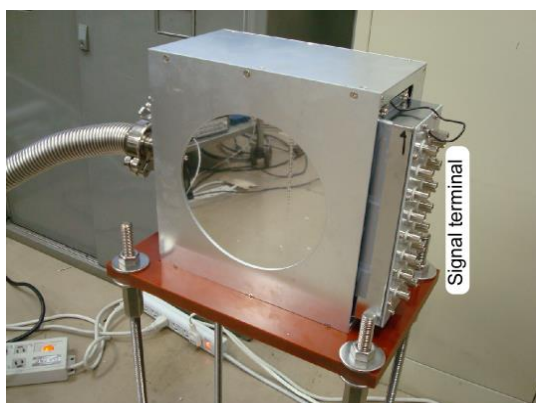


Figure 1 NMIJ graphite calorimeter

coefficients of the field at NMIJ were $\sim 0.4\%$ smaller than those at BIPM. These differences are within the combined uncertainties (0.46%).

Calibration services to end users in hospitals have started from October 2012 through a secondary calibration laboratory in the framework of the Japan Calibration Service System (JCSS), where the calibration laboratory needs to satisfy the requirements of ISO/IEC 17025. By this traceability system, end users can be expected to improve the standard dose uncertainty from 2.3% to 1.5% for high-energy photon beams from a clinical linac.

2-2. Effect of Build-up Cap on the Signal Current from an Ionization Chamber

It was shown in ref. [3] that positive charges are accumulated in a PMMA build-up cap irradiated in a high-energy photon field, and as a result, the signal current decreases in spite of the constant dose irradiation. To evaluate the dissipation time of the accumulated charges, we intermittently irradiated an ionization chamber with a build-up cap, which had accumulated positive charges [4]. The dots plotted for $t < 24$ h in Figure 2 show the output current (half-life corrected) from an ionization chamber irradiated continuously with cobalt 60 gamma rays. The output current decreases with time (dose) due to the charge accumulation. The dots plotted for $t > 24$ h in Figure 2 show the output current from the ionization chamber irradiated intermittently, i.e., repeating current measurements under irradiation for 200 s and non-irradiation for 2000 s. The output current increases slowly due to the charge dissipation. From an analysis that assumes a simple charge dissipation process, the dissipation time is evaluated to be ~ 200 h.

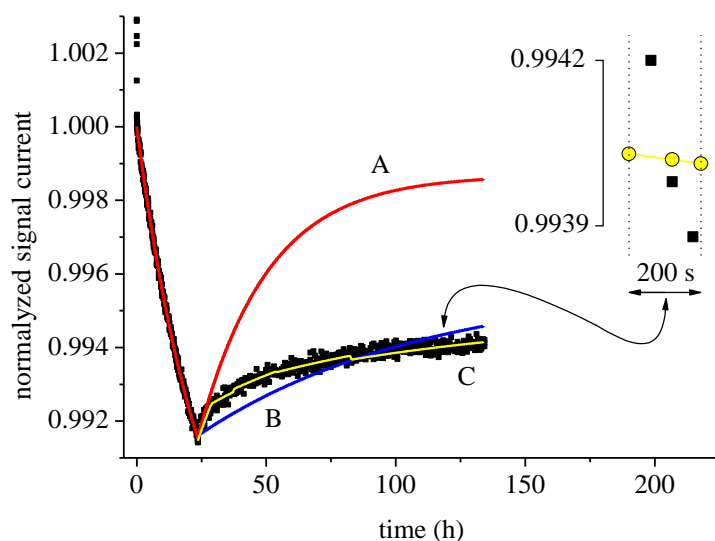


Figure 2 Normalized signal current from an ionization chamber irradiated continuously ($t < 24$ h), and intermittently ($t > 24$ h). The dots denote the experimental

results and the curves A, B, and C are calculation results obtained using models. See Ref.[4] for details on the models.

2-3. Mammography radiation quality [5, 6, 7]

NMIJ developed the air kerma standards for mammography radiation with Rh/Rh target/filter combination in July 2012. The air kerma standards for mammography radiation in three types of target/filter combinations (Mo/Mo, Mo/Rh, and Rh/Rh) are disseminated. A glass dosimeter (Figure 4), which was specially designed for the mean glandular dose (MGD) evaluation at hospitals, has been evaluated using these radiation qualities. The glass dosimeters are used for quality control of mammography in many hospitals. The distribution of MGD in 2010, which was obtained by use of the glass dosimeters, is shown in Figure 5.

New radiation qualities of W/Rh, W/Ag, and W/Al are used in digital mammography and breast tomosynthesis units. NMIJ develops air kerma standards for these radiation qualities. The shielding box for mammography X-ray tubes was modified to mount a new tungsten target X-ray tube (see Figure 3). The progress in the development of the air kerma standards for mammography radiation is summarized in Table 1.

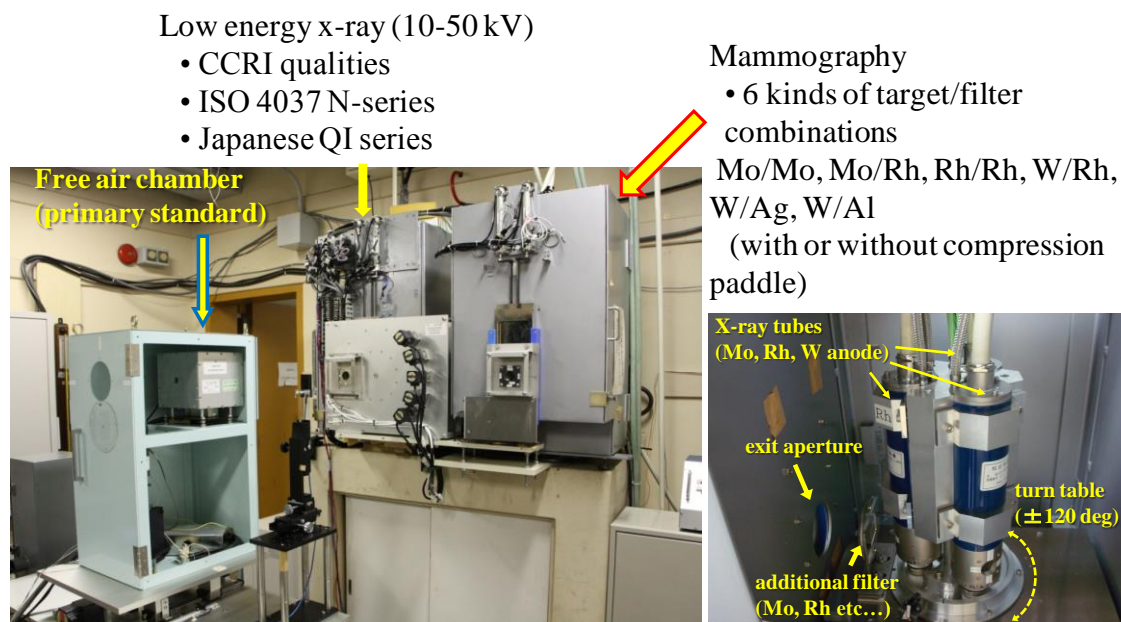


Figure 3 Photograph of the low-energy and mammography X-ray calibration facility.

Table 1 Progress in the development of the mammography X-ray air kerma standards.

target/filter	status
Mo/Mo (30, 32 μm)	Disseminated (Mar. 2009)
Mo/Rh (25 μm)	Disseminated (Mar. 2011)
Rh/Rh (25 μm)	Disseminated (Jul. 2012)
W/Rh (50 μm)	Evaluation completed
W/Ag (50 μm)	Under construction
W/Al (0.5, 0.7 mm)	Under construction

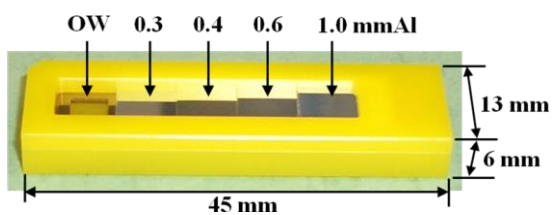


Figure 4 Picture of a glass dosimeter specially designed for measuring mammography radiation (in cooperation with Chiyoda Technol. Corporation).

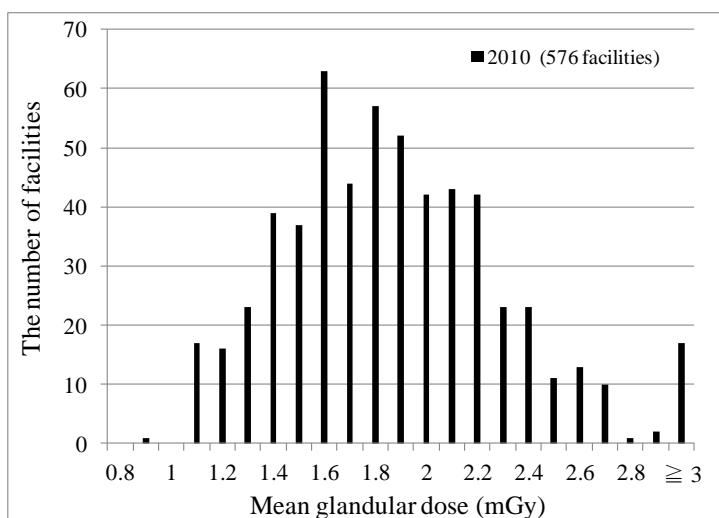


Figure 5 Distribution of the mean glandular dose evaluated by use of the glass dosimeters in 2010 [7].

2-4. Clinical linac

(1) Absorbed dose to water in high-energy photon beams

We have been developing a standard for absorbed dose to water in a high-energy photon beam using the graphite calorimeter, which is used for the standard for absorbed dose to water in a Co-60 gamma-ray field. The high-energy photon beams are provided by the clinical linac (Figure 6) installed at NMIJ in the beginning of 2010. The nominal energies of the photon beams are 6, 10, and 15 MV. The beam quality indexes of the photon beams are listed in Table 2.



Figure 6 Clinical linac and 3D water phantom

Table 2 Beam quality index of the clinical linac at NMIJ

Nominal Energy	$TPR_{20,10}$	
	Exp.	Calc.
6 MV	0.678	0.679
10 MV	0.728	0.731
15 MV	0.758	0.760

In order to determine the conversion factor from the absorbed dose to graphite to that to water, we have calculated the beam characteristics of the high-energy photon beams from the clinical linac using the Monte Carlo code, EGS5. To reduce the statistical uncertainties of the beam characteristics and conversion factor, we developed EGS5-MPI as an extended package of EGS5 for parallelization using a message passing interface (MPI) implementation. Our calculation and experimental results of $TPR_{20,10}$ and percentage dose distribution (PDD) of the 10 MV photon beam are given in Table 2 and Figure 7, respectively. The PDD calculation results of the 10 MV photon beam agrees well with the experimental results.

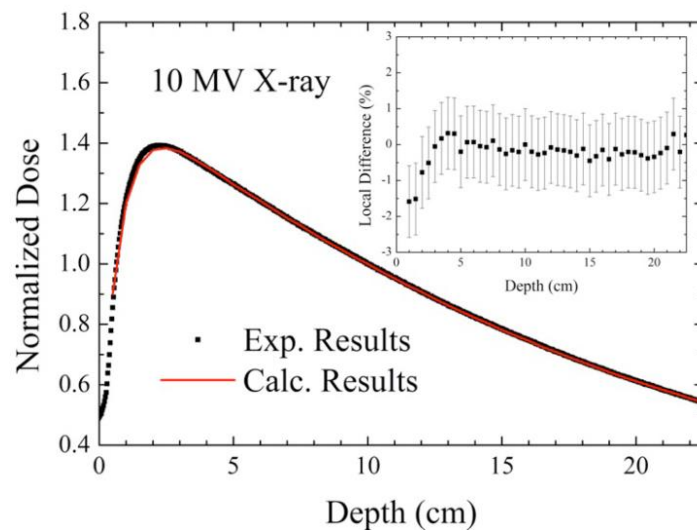


Figure 7 Percentage dose distribution of the 10 MV photon beam. The experimental results are shown as dots. The red line shows calculation results.

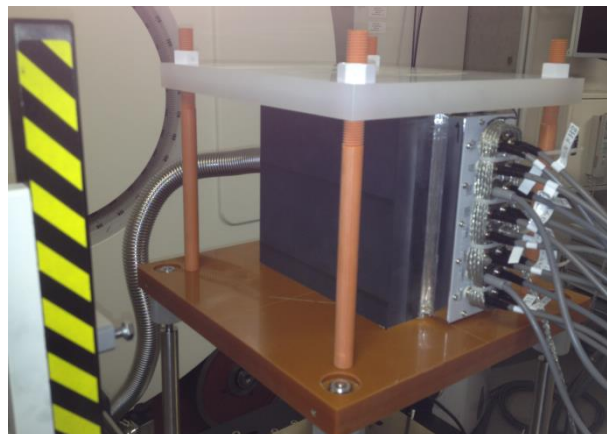


Figure 8 The graphite calorimeter. For protection from large earthquakes, the calorimeter and the graphite plates are fixed on a calorimeter stage.

The graphite calorimeter determines the absorbed dose to graphite. Figure 8 shows the graphite calorimeter. The reference distance from the source and the reference depth in water are 1 m and 10 g/cm^2 , respectively. The reference depth can be modified with the use of additional graphite plates.

The absorbed dose to graphite is determined from the bridge output of the thermistor in the calorimeter core. Figure 9 shows the bridge output for the 10 MV photon beam irradiation. The bridge output voltage of the graphite core increases when the temperature of the graphite core is increased by the photon beam irradiation. We also heat the graphite core using a thermistor in the graphite core. The absorbed dose to graphite is determined by comparing the temperature increase with the heater.

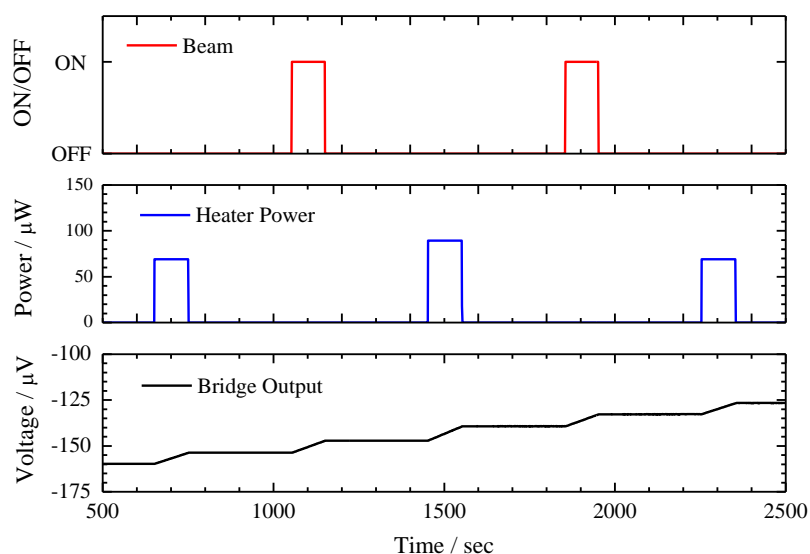


Figure 9 Bridge output of the graphite core (solid line), photon beam ON/OFF signal (red line), and the external heater power in the core (blue line).

We determine the calibration coefficient ($N_{w,Q}$) and beam quality correction factor (k_Q) of the waterproof farmer type ion chamber (PTW type 30013) by using the graphite calorimeter. The calibration coefficient and beam quality correction factor are given in Table 3, and Figure 10 shows the comparison of the beam quality correction. The beam quality correction factor for the 10 and 15 MV photon beams are in good agreement with the calculation data for each dosimetry code (TRS-398, JSMP01 and JSMP12). We plan to start the calibration service in this year and to perform the bilateral comparison with the ARPANSA in May, 2013. The results will be reported elsewhere soon after the comparison.

Table 3 Calibration coefficients and beam quality correction factors of the farmer-type ion chamber (PTW type 30013).

Nominal Energy	$TPR_{20,10}$	$N_{w,Q} / \text{Gy nC}^{-1}$	k_Q
Co-60 γ	-	0.05370	-
6 MV	0.678	0.05293	0.9856
10 MV	0.728	0.05266	0.9807
15 MV	0.758	0.05216	0.9713

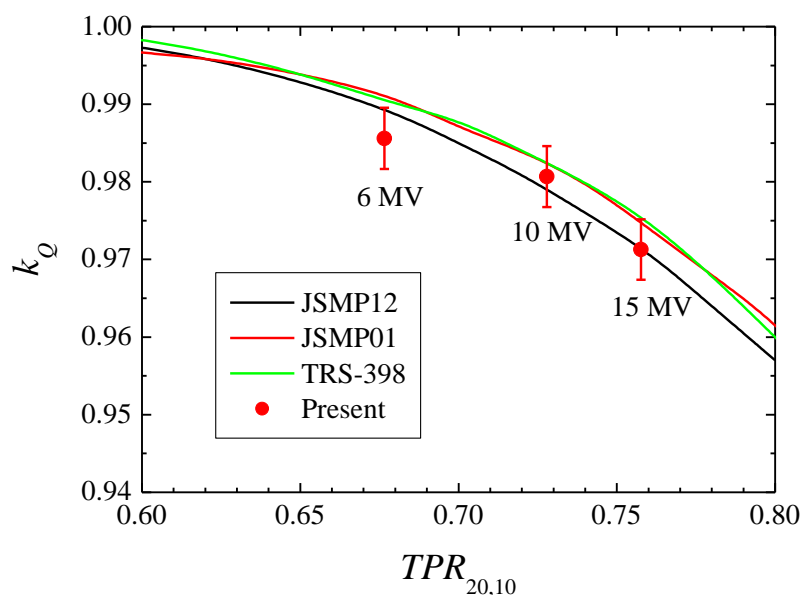


Figure 10 Comparison of the beam quality correction factor (k_Q) for a farmer-type ion chamber (PTW type 30013). The black and red curves show the k_Q data from the Japanese dosimetry protocols (Black: JSMP01[8], Red: JSMP12[9]). The k_Q data from TRS-398 is also shown as a green curve [10].

(2) Absorbed dose to water in high-energy electron beams

The clinical linac can produce electron beams with energies of 6, 9, 12, 15, 18, and 22 MeV. The reference depth for measuring the absorbed dose depends on the electron beam energies. The reference depth for the electron beam is thinner than that of the clinical photon beams. A new graphite calorimeter with a thin graphite entrance window has been designed and is currently under construction (Figure 11).

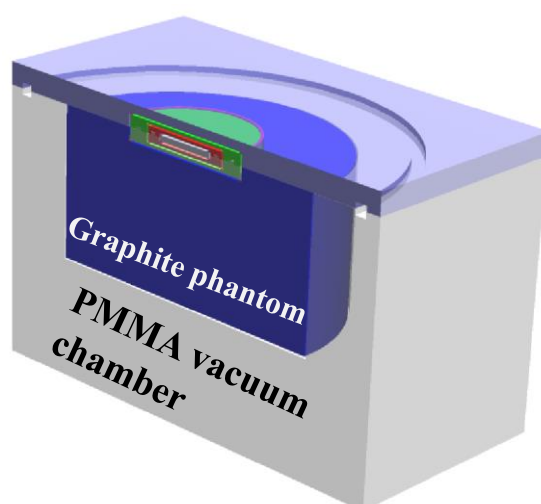


Figure 11 A schematic image of the new graphite calorimeter with a thin graphite entrance window.

2-5. Reference air kerma rate for an Ir-192 brachytherapy source

The standard of reference air kerma rate for an Ir-192 brachytherapy source is being developed in collaboration with the Japan Radioisotope Association. A cylindrical graphite cavity chamber is used for the air kerma measurement. The photon spectrum for Ir-192 was measured using a Ge detector with a narrow collimator for the evaluation of several correction factors. The photon spectrum was evaluated by the unfolding method with the response function calculated by EGS5. Figure 12 shows the measured and unfolding spectrum. We plan to start the calibration service in 2014.

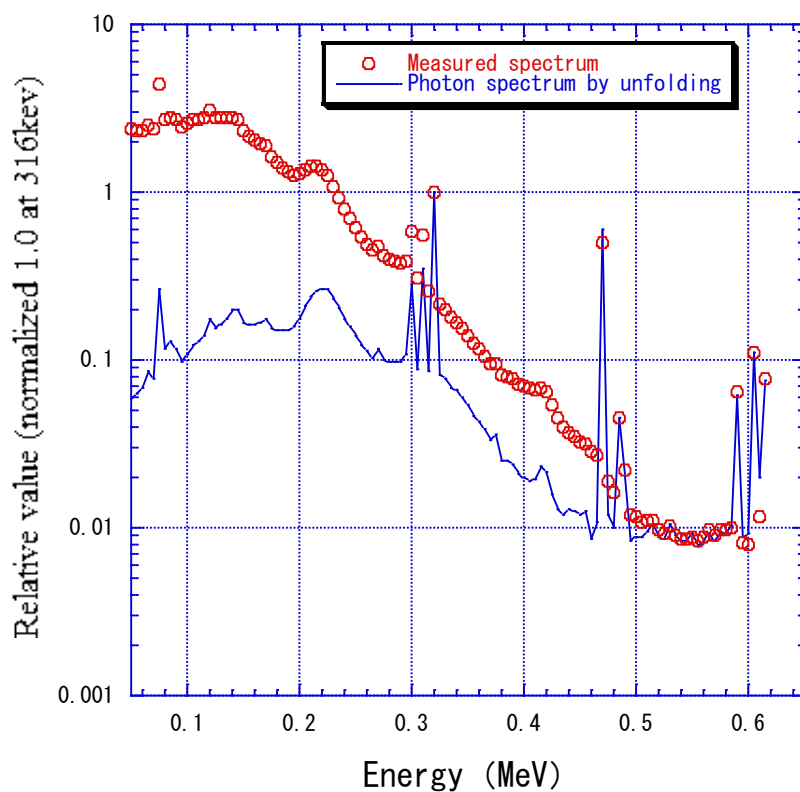


Figure 12 The measured and unfolding spectrum for an Ir-192 brachytherapy source using a Ge detector.

2-6. Air kerma for Co-60 and Cs-137 gamma rays

The air kerma standards for the Co-60 and Cs-137 gamma rays at NMIJ were peer-reviewed in October 2008, and the ISO17025 quality system was established in 2004. Our largest Co-60 gamma-ray source, 148 TBq, was replaced by a new one last January. The range of air kerma rate and calibration and measurement capability ($k=2$) are listed in Table 4.

Table 4 Range of air kerma rate and calibration and measurement capability ($k=2$)

Source	Range of air kerma rate (Gy/s)	Calibration and measurement capability ($k=2$)
Co-60 γ -rays	$1.6 \times 10^{-9} - 1.5 \times 10^{-1}$	1.0% at 1.3×10^{-2} Gy/s
Cs-137 γ -rays	$5.8 \times 10^{-10} - 4.4 \times 10^{-4}$	0.8% at 6.6×10^{-4} Gy/s

2-7. Dose equivalent for Co-60 and Cs-137 gamma rays

The ambient, directional and personal dose equivalent were evaluated for the ^{60}Co and ^{137}Cs gamma rays by measured photon spectra. Conversion coefficient and calibration and measurement capability ($k=2$) are listed in Table 5.

Table 5 Conversion coefficient for and calibration and measurement capability ($k=2$)

Source	H*(10) (Sv/Gy)	H*(0.07) (Sv/Gy)	Hp(10) (Sv/Gy)	Hp(0.07) (Sv/Gy)	Calibration and measurement capability ($k=2$)
Co-60 γ -rays	1.16	1.16	1.15	1.17	3 %
Cs-137 γ -rays	1.20	1.21	1.22	1.22	3 %

2-8. Air kerma for medium-energy X-rays (50 kV – 300 kV)

The air kerma standards for medium-energy X-rays at NMIJ were peer-reviewed in October 2008, and the ISO17025 quality system was established in June 2005. The range of air kerma rate and calibration and measurement capability ($k=2$) are listed in Table 6.

Table 6 Range of air kerma rate and calibration and measurement capability ($k=2$)

X-ray quality	Range of air kerma rate (Gy/s)	Calibration and measurement capability ($k=2$)
BIPM quality (ISO 4037-1) Narrow spectrum Low kerma rate High kerma rate Wide spectrum Japanese QI series	$9.0 \times 10^{-9} - 2.0 \times 10^{-3}$	1.2% at 2.7×10^{-4} Gy/s

The qualities of X-rays provided are BIPM quality, 4 qualities in ISO4037 and Japanese QI (quality index, $E_{\text{eff}}/E_{\text{max}}$), where E_{eff} is the effective X-ray energy and E_{max} is the maximum X-ray energy.

2-9. Air kerma for low-energy X-rays (10 kV – 50 kV)

The air kerma standards for low-energy X-rays at NMIJ were peer-reviewed in October 2008, and the ISO17025 quality system was established in June 2005. The range of air kerma rate and the calibration and measurement capability ($k=2$) are listed in Table 7.

Table 7 Range of air kerma rate and calibration and measurement capability ($k=2$) of low energy X-rays

Radiation quality	Range of air kerma rate (Gy/s)	Calibration and measurement capability ($k=2$)
<ul style="list-style-type: none"> • BIPM quality • ISO 4037 Narrow spectrum series • Japanese QI series 	$2.5 \times 10^{-6} - 1.0 \times 10^{-2}$	0.8% at 4.4×10^{-5} Gy/s

NMIJ acts as a pilot laboratory in the APMP comparison of the national air kerma standards for low energy X-rays (APMP.RI(I)-K2). The participants are Nuclear Malaysia (Malaysia), BARC (India), ARPANSA (Australia), INER (Chinese Taipei), OAP (Thailand), AEC (Syria), and IAEA and NIM (China). The comparison started in August 2008 and ended in May 2011. The Draft B report is under review.

2-10. Absorbed dose to tissue for beta-particle radiation

The standards of absorbed dose to tissue at a depth of 0.07 mm for beta particles emitted from Sr-90/Y-90, Kr-85, and Pm-147 were established and a calibration service for the area and personal dosimeters in these radiation fields were offered in 2006. The ISO17025 quality system was established in March 2009. The beta-particle irradiation system (Figure 13), which was damaged by the earthquake disaster in March 2011, has been recovered in March 2012. The system, after repair, shows the same performance as before. The absolute values of the absorbed dose rate determined by an extrapolation chamber and calibration and measurement capability ($k=2$) are listed in Table 8. We, as a pilot laboratory, have started an APMP comparison of the standards. Further, we plan to establish a standard for brachytherapy sources (Ru-106) for eye applicators.

Table 8 The absorbed dose rate to tissue and calibration and measurement capability.

	Reference absorbed dose rate (Gy/s)	Uncertainty ($k=2$)
⁹⁰ Sr/ ⁹⁰ Y with a beam flattening filter at the distance of 30 cm	1.1×10^{-5}	2.8%
⁸⁵ Kr with a beam flattening filter at the distance of 30 cm	3.8×10^{-5}	2.8%
¹⁴⁷ Pm with a beam flattening filter at the distance of 20 cm	2.0×10^{-6}	4.8%

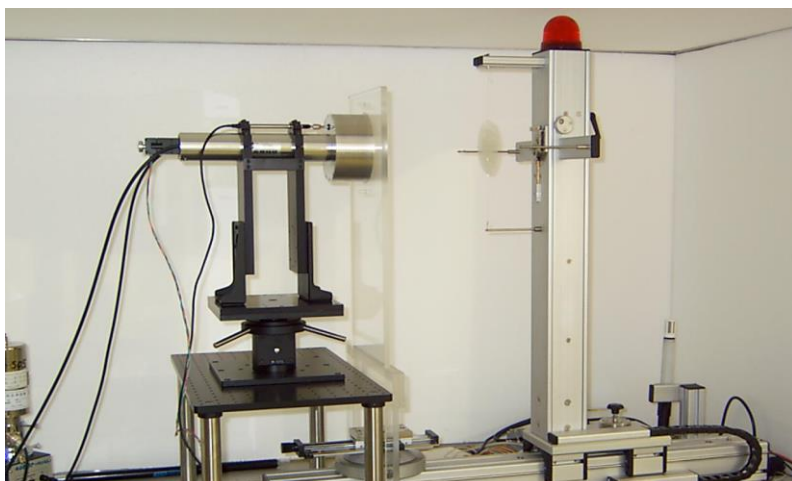


Figure 13 An extrapolation chamber and a beta-ray irradiation system.

2-11. Pulse energy for X-ray (4-20 keV) free electron laser

The Japanese hard X-ray free-electron laser (XFEL), SACLA (SPring-8 Angstrom Compact free-electron Laser, Figure 14), the world's second hard XFEL after LCLS (the Linac Coherent Light Source) in the USA, can provide coherent, high intensity, ultra-short femtosecond X-ray pulses with a photon energy larger than 10 keV. The pulse energies of a free electron laser have been accurately measured in the hard X-ray spectral range using a cryogenic radiometer with an uncertainty of 1–4%. **Figure 15** shows the schematic diagram of the beamline in SACLA and the cryogenic radiometer. The cavity absorber in the radiometer consists of an absorber with a 1.0 mm-thick gold base and a 0.1 mm-thick cylindrical shell made of copper (Au/Cu cavity absorber). In the photon energy regime from 4.4 keV to 16.8 keV, pulse energies of up to 100 μJ were obtained at the new hard X-ray laser facility, SACLA [11].



Figure 14 X-ray FEL facility (SACLA).

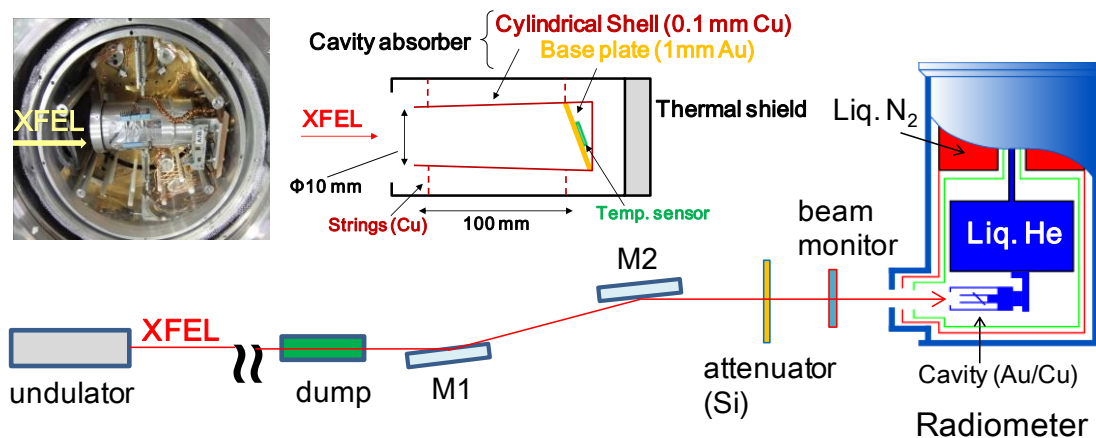


Figure 15 A schematic diagram of the beamline at SACLA and the cryogenic radiometer.

3. Field photon energy spectra in Fukushima after the nuclear accident

After the accident at the Fukushima Dai-ichi Nuclear Power Plant, radionuclides spread over a large area. Cs-137 and Cs-134 nuclei are now the main sources of gamma rays. The field gamma-rays, however, are not of the mono-energy type because they contain photons scattered from the ground, air, etc. The corresponding photon energy spectra have been measured using a CdZnTe detector (GR1), manufactured by Kromek, at several points in Fukushima to evaluate the reference energy spectra after the nuclear accident. The decontamination of the radioactive material is ongoing for houses, parks, roads, farmland, etc. It is expected that the photon energy spectrum will change after the decontamination, and hence, the measurement points in the present study are selected to be both in non-decontaminated and decontaminated areas, as listed in

Table 9.

The results are shown in Figure 16. They are all normalized at the peak, which corresponds to the Cs-137 gamma ray, i.e., 662 keV. The spectrum obtained at point C is different from other obtained spectra in the low energy region. It is clear that the energy spectrum of the field photons changes upon decontamination around the measurement point. The percentage of Cs-134 and Cs-137 gamma rays decreases upon decontamination. It is possible that the primary gamma rays of Cs-137 and Cs-134 that are detected are only from near areas (several tens of meters) and the scattered photons are from distant areas. This indicates that air might be working as a scattering material.

Table 9. Information about measurement points

	Ambient dose rate ($\mu\text{Sv/h}$)	Information
Point A	6.0	Road side in Iidate village. There is no decontamination area around this point
Point B	3.7	Point in large flat field (100 m \times 50 m) at Iidate village. There is no decontamination area around this point.
Point C	0.4	Point in large flat decontaminated field (100 m \times 50 m) at Iidate village.
Point D	0.86	Point at Fukushima city near Fukushima station.

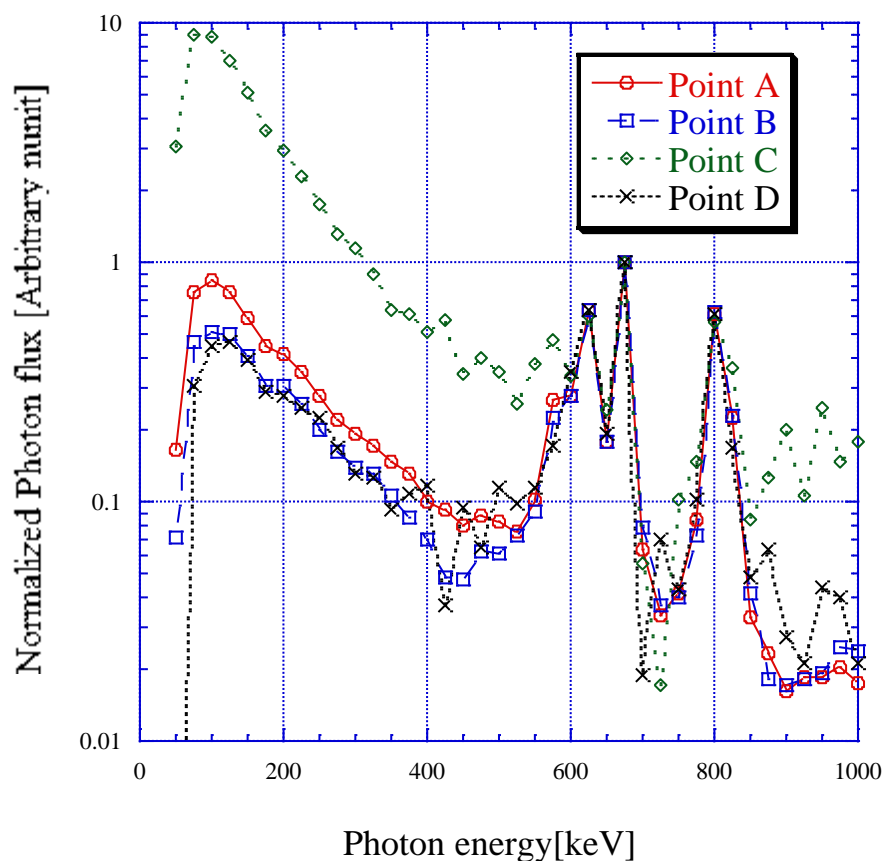


Figure 16 Normalized photon flux at each point. Flux is normalized at the peak of the Cs-137 gamma rays.

References

1. Y. Morishita, M. Kato, N. Takata, T. Kurosawa, T. Tanaka and N. Saito., Radiat. Prot. Dosim. doi:10.1093/rpd/ncs235.
2. C. Kessler, P. J. Allisy-Roberts, Y. Morishita, M. Kato, N. Takata, T. Kurosawa, T. Tanaka and N. Saito, Metrologia, 48 06008 (2011).
3. N. Takata and Y. Morishita, Radiat. Prot. Dosim., 145 21-27 (2011).
4. Y. Morishita and N. Takata, Radiat. Prot. Dosim., doi:10.1093/rpd/nct006.
5. T. Tanaka, T. Kurosawa, R. Nouda, T. Matsumoto, N. Saito, S. Matsumoto, K. Fukuda, Proceedings of the International Symposium on Standards, Applications and Quality Assurance in Medical Radiation Dosimetry (IDOS), 2, 43-51 (2011).
6. C Kessler, D T Burns, T Tanaka, T Kurosawa and N Saito, Metrologia 47, 06024 (2010)
7. S. Matsumoto, FBNews, No. 416, 12-16 (2011) (in Japanese).
8. JSMP, Standard Dosimetry of Absorbed Dose in External Beam Radiotherapy (Standard Dosimetry 01), JSMP, 2001.
9. JSMP, Standard Dosimetry of Absorbed Dose to Water in External Beam Radiotherapy (Standard Dosimetry 12), JSMP, 2012.
10. IAEA, Absorbed Dose Determination in External Beam Radiotherapy, Technical Report Series 398, IAEA, Vienna, 2000.
11. M. Kato, T. Tanaka, T. Kurosawa, N. Saito, M. Richter, et al., Applied Physics Letters **101**, 023503 (2012).